Exploring Localization in Nuclear Spin Chains

Exploring Localization in Nuclear Spin Chains

Ken Xuan Wei,[1] Chandrasekhar Ramanathan,[2] and Paola Cappellaro[3,*]
[1]Department of Physics and Research Laboratory of Electronics, Massachusetts Institute of Technology, Cambridge, Massachusetts 02139, USA
[2]Department of Physics and Astronomy, Dartmouth College, Hanover, New Hampshire 03755, USA
[3]Department of Nuclear Science and Engineering and Research Laboratory of Electronics, Massachusetts Institute of Technology, Cambridge, Massachusetts 02139, USA

(Received 26 July 2017; published 12 February 2018)

Characterizing out-of-equilibrium many-body dynamics is a complex but crucial task for quantum applications and understanding fundamental phenomena. A central question is the role of localization in quenching thermalization in many-body systems and whether such localization survives in the presence of interactions. Probing this question in real systems necessitates the development of an experimentally measurable metric that can distinguish between different types of localization. While it is known that the localized phase of interacting systems [many-body localization (MBL)] exhibits a long-time logarithmic growth in entanglement entropy that distinguishes it from the noninteracting case of Anderson localization (AL), entanglement entropy is difficult to measure experimentally. Here, we present a novel correlation metric, capable of distinguishing MBL from AL in high-temperature spin systems. We demonstrate the use of this metric to detect localization in a natural solid-state spin system using nuclear magnetic resonance (NMR). We engineer the natural Hamiltonian to controllably introduce disorder and interactions, and observe the emergence of localization. In particular, while our correlation metric saturates for AL, it slowly keeps increasing for MBL, demonstrating analogous features to entanglement entropy, as we show in simulations. Our results show that our NMR techniques, akin to measuring out-of-time correlations, are well suited for studying localization in spin systems.

DOI: 10.1103/PhysRevLett.120.070501

Anderson first demonstrated that single particle wave functions can become exponentially localized in the presence of disorder [1]. Whether this localization [2–4] survives in the presence of interactions has received much attention in recent years [5–10]. Numerical evidence in spin chains indicates that the system may be in the many-body localization (MBL) or ergodic phase depending on the relative strength of interaction and disorder [11–13]. MBL can be distinguished from its noninteracting counterpart [Anderson localization (AL)] via the dynamics of entanglement entropy [14–17]. Entanglement entropy (EE) is, however, difficult to evaluate experimentally and so far has only been measured on systems with a small number of particles [18]. One way to circumvent this challenge is to measure entanglement witnesses such as the quantum Fisher information, which can serve as a lower bound for entanglement entropy [8] for pure states.

A remarkable feature about the MBL phase is that it is predicted to persist at high and even infinite temperature [19], where states are highly mixed and there is little to no entanglement present. How does one characterize the MBL phase experimentally in such a system? Here, we introduce a novel metric capable of distinguishing MBL from AL in the nonequilibrium dynamics of highly mixed states and provide both numerical and experimental evidence in support. Our approach requires no local control and relies only on collective rotations and measurements, in contrast to recently proposed metrics [20] that also detect the spread of correlations, but require single-spin addressability. The experimental system is composed of nuclear spins in a natural crystal coupled by the magnetic dipolar interaction, which can be mapped with high fidelity to an ensemble of 1D, nearest-neighbor coupled spin chains [21,22]. We exploit Hamiltonian engineering techniques to selectively introduce and tune both the interaction strength and the degree of disorder in the system, and measure the growth of many-spin correlations in both the AL and MBL regimes.

We consider a linear chain of L spins initially at equilibrium at high temperature ($\beta \to 0$) in a strong magnetic field aligned along the $\hat{z}$ direction. Under these conditions, the thermal equilibrium state of the system can be expressed $\rho_{\mathrm{eq}} = (\mathbb{1} - \epsilon \sum_j S_z^j)/2^L$ (with S as the spin-1/2 operator) to first order in $\epsilon = \beta\omega_L \ll 1$, where ω_L is the spin Zeeman energy and $\hbar = 1$. Any spin-spin interactions are assumed to be negligible compared to the Zeeman energy, so that the natural interaction Hamiltonian commutes with the thermal equilibrium state.

If the effective interaction Hamiltonian H of the system is changed suddenly (a rapid quench), the system is no longer in equilibrium and evolves into a many-body correlated state. The presence of disorder hinders the growth of correlations and can give rise to localized states, characterized by an exponentially decreasing probability of

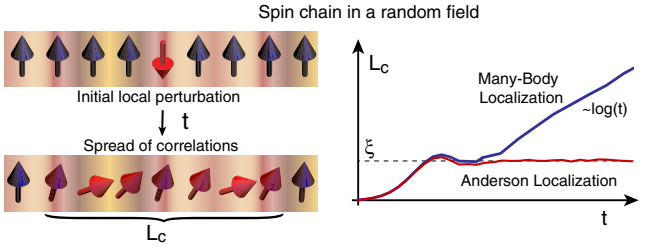

FIG. 1. Quantum many-body correlations grow from an initial localized state, but are restricted to a finite size by disorder. The average correlation length L_c, which measures the spread of the correlations, saturates at the localization length ξ in the case of AL, but grows logarithmically with time in the MBL regime.

correlations outside a typical localization length ξ, as shown in Fig. 1. Inspired by this picture, we define a metric of localization that measures the average length over which correlations have developed.

We can generically write the high-temperature time-evolved density matrix as

$$\rho(t) = \frac{\mathbb{1}}{2^L} - \frac{\epsilon\sqrt{L}}{2^L}\sum_{k=1}^{L}\sum_{s=1}^{\zeta_k} b_k^s(t)\mathcal{B}_k^s, \tag{1}$$

where $\mathcal{B}_k^s$ are operators composed of tensor products of k Pauli matrices and $L-k$ identity operators. Here, ζ_k is the number of configurations with exactly k nonidentity Pauli operators. To quantify localization we define the "average correlation length"

$$L_c = \sum_{k=1}^{L} k f_k, \tag{2}$$

where $f_k = \sum_{s=1}^{\zeta_k}[b_k^s]^2$ is the contribution of all possible spin correlations with Hamming weight k (with $\sum_{k=1}^{L} f_k = 1$). In the initial equilibrium state ρ_{eq} there are no spin correlations and $L_c = 1$. In the absence of disorder, we expect L_c to grow and eventually saturate at a value dependent on L. Introducing disorder leads to a quantitatively different behavior. When the system is noninteracting, AL leads to a coherent suppression of many-spin correlations and L_c is bound by the localization length ξ. When interactions are present, disorder is unable to completely suppress the correlation growth. The slow growth of L_c in the presence of interactions is the key feature that enables L_c to distinguish between AL and MBL for mixed states.

Consider an effective spin Hamiltonian of the form

$$H = \frac{u+v}{2}\sum_{j=1}^{L-1} JS_x^jS_x^{j+1} + \frac{v-u}{2}\sum_{j=1}^{L-1} JS_y^jS_y^{j+1} + g\sum_{j=1}^{L} h_jS_z^j - v\sum_{j=1}^{L-1} JS_z^jS_z^{j+1}. \tag{3}$$

The first two terms represent an integrable Hamiltonian, as they map to a free fermionic Hamiltonian via a Jordan-Wigner transformation [23]. The third term corresponds to on site disorder, and the last term introduces interactions between fermions (see Sec. 2 in the Supplemental Material [24], which includes Refs. [25–41]). Tuning the relative strength of these parameters allows us to explore different physical regimes. Figure 2 shows that both EE ($S = -\mathrm{Tr}[\rho_L \log \rho_L]$, where ρ_L is the reduced density matrix of the left half of the chain) and the correlation length L_c display a characteristic logarithmic growth in time [15] when the system enters the MBL phase and saturate when the system is noninteracting. These numerical simulations suggest that L_c can be used as an alternative to EE to distinguish MBL from AL for mixed states (Sec. 6.3 of the Supplemental Material [24]). L_c and EE are related for more general states that arise from evolution under other spin Hamiltonians.

Measuring L_c for a generic many-body state is challenging, since it is usually difficult to directly measure many-body correlations to determine f_k, and the number of configurations ζ_k is exponential in k and L. Here, we show how to extract L_c in our experiments, with a method that can be extended to other systems.

Our experimental system consists of a single crystal of fluorapatite [$Ca_5(PO_4)_3F$] placed in a strong magnetic field (7 T, $\omega_L = 283$ MHz). The ^{19}F spin-1/2 nuclei in the hexagonal fluorapatite crystal form linear chains along the c axis, interrupted only by rare defects, each surrounded by six other chains. When the c axis is oriented parallel to the external magnetic field, the cross-chain couplings is 40 times weaker than nearest-neighbor intrachain couplings ($J = -33$ krad/sec). The system can then be treated approximately as an ensemble of identical spin chains

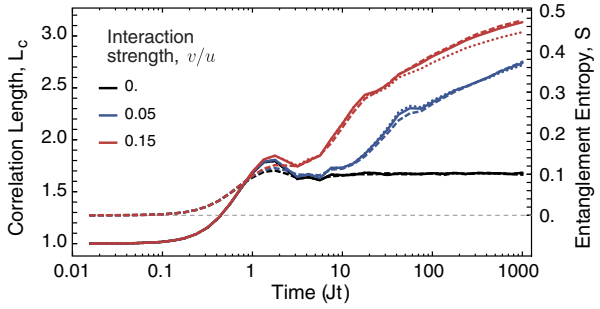

FIG. 2. Simulations of spin correlation and entanglement entropy. We compare EE of the reduced half chain (dashed lines, right axis) with the correlation length L_c (solid lines, left axis) and the approximate L_c obtained from measuring the MQC (dotted). Simulations using exact diagonalization were performed for $L = 8$ and with a uniform random noise $gh_j/u \in [-8, 8]$ for 960 realizations. The similar behaviors (including logarithmic growth) confirm that L_c is as good an indicator of MBL as the more commonly used EE. Here, EE is renormalized to vary between zero and one, in order to account for the mixed initial state of the system (Sec. 6 of Supplemental Material [24]).

[22,42,43]. In addition, each F spin is surrounded by three ^{31}P spin-1/2 nuclei. The spins interact via the natural dipolar Hamiltonian, $H_{\rm nat} = \frac{1}{2}\sum_{j<k} J_{jk}(2S_z^j S_z^k - S_x^j S_x^k - S_y^j S_y^k) + \sum_{j,\kappa} h_{j\kappa} S_z^j s_z^\kappa$, where $S_\alpha^j = \sigma_\alpha^j/2$ ($\alpha = x, y, z$) are spin-1/2 operators of the jth F spin and s_z^κ of the κth P spin.

At room temperature, the P spins are in an equal mixture of $m_z = \pm 1/2$ states. This allows us to replace the heteronuclear interactions by $\sum_j h_j S_z^j$, where h_j is now a random variable representing the disordered field seen locally by each ^{19}F. The dipolar coupling between ^{31}P nuclei is about 27 times smaller than that between ^{19}F nuclei and can be neglected on our experiment time scales. The random local field thus appears quasistatic in these experiments, resulting in an effective Hamiltonian $H_{\rm nat}^{\rm eff} = (J/2)\sum_j (2S_z^j S_z^{j+1} - S_x^j S_x^{j+1} - S_y^j S_y^{j+1}) + \sum_j h_j S_z^j$, where we kept nearest-neighbor couplings only.

While the high-temperature thermal equilibrium state does not evolve under this Hamiltonian, we can quench the system to a different effective Hamiltonian of the form of Eq. (3) by periodically applying a radio frequency (rf) pulse sequence in resonance with the F spins. This method (called coherent averaging [44]) has been long used in the nuclear magnetic resonance (NMR) literature for spectroscopy and condensed matter studies. Here, we further push these techniques to engineer the broad class of Floquet (periodic) Hamiltonians in Eq. (3), with tunable disorder and interactions. Changing the sequences of pulses and delays in a period, we can experimentally adjust the parameters u, v, and g and explore various regimes of interest (Sec. 3.2 in the Supplemental Material [24] shows the experimental pulse sequence). In addition, we are also able to reverse the arrow of time, a tool that allows measuring out-of-time ordered correlations (OTOCs).

In order to calculate the correlation length L_c, we need the coefficients f_k, which we can determine experimentally by borrowing from well-known NMR techniques that approximate the number of correlated spins by their quantum coherence number [45]. Multiple quantum coherence (MQC) intensities of order q describe the contribution of terms $|m_a\rangle\langle m_a'|$ in the density matrix, such that $m_a - m_a' = q$, with m_a the collective S_a eigenvalue (typically $a = z$). MQC intensities I_q can be measured by relying on their distinct behavior under collective rotations [45–47]. The distribution of I_q has been traditionally used to approximate the average number of correlated spins in 3D spin networks [48–50]. While this approximation fails in 1D systems, we find instead a practical experimental protocol to *exactly* measure L_c for noninteracting systems. The protocol still yields a very good approximation for disordered interacting (MBL) systems.

We first note that, in noninteracting systems, for simple initial states such as $\rho_{\rm eq}$, the density operator at time t, when expanded in the form of Eq. (1) has a particularly simple form. The number of configurations with k Pauli operators, $\zeta_k \propto L - k$, as all many-spin correlations are of the form $\mathcal{B}_k^s \sim S_a^s(\prod_{l=s+1}^{k+s-2} S_z^l) S_b^{k+s-1} \pm S_b^s(\prod_{l=s+1}^{k+s-2} S_z^l) S_a^{k+s-1}$, where the end spins $S_{a,b}$ are either S_x or S_y. This structure is key to extracting the f_k coefficients, as correlations with different k will exhibit distinct MQC intensities. To further distinguish the four different end-spin combinations, we first decompose $\rho(t)$ into four corresponding orthogonal blocks, using time reversal and phase cycling [51], and then measure the MQC intensities encoded in the x axis for each jth block, I_q^j (see Sec. 5 in the Supplemental Material [24]). The resulting MQC intensities can be related to f_k in Eq. (2) by a linear transformation, $f_k = \sum_{jq} M_{kq}^{(j)} I_q^j$, and from the extracted f_k we can calculate L_c. While this protocol was designed for the Hamiltonian we investigated, similar strategies will be available for other integrable Hamiltonians, with a proper choice of the axes along which the MQC are measured.

As long as the interaction term is not too large (and disorder large enough), we expect the evolved density matrix state to still mostly contain the simpler many-spin correlations described above, thus allowing us to extract an approximate L_c. The validity of this argument can be seen from the simulation results shown in Fig. 2, where the approximated L_c (calculated from the MQC) continues to closely track the exact L_c and the entanglement entropy in the MBL phase.

Combining Hamiltonian engineering with MQC readout, we can explore the behavior of both noninteracting and interacting models in the presence of disorder. Figure 3 shows the experimentally extracted L_c for our interacting model, as compared to the noninteracting case. For the noninteracting Hamiltonian ($v = 0$), in the absence of disorder, we expect L_c to increase linearly, consistent with

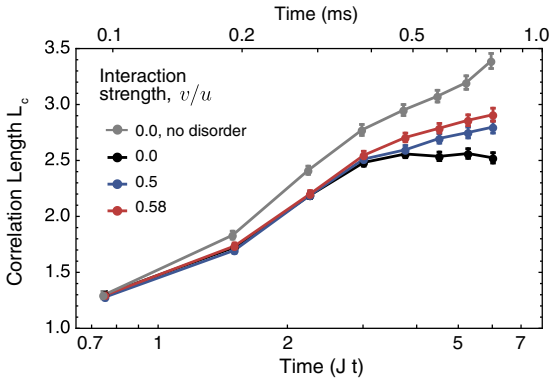

FIG. 3. Experimental measurements of correlations in interacting spin chains. We plot in log-linear scale the L_c dynamics for varying interaction strengths v, in the presence of disorder. Data are for $u = 0.24$ and $g = 0.12$. After an initial growth of correlations, L_c saturates for the noninteracting systems, while it shows a slow growth in the presence of interactions, indicating MBL. In contrast, the integrable case (gray, $v = 0$, $g = 0$) shows more pronounced growth, although it is still limited by experimental imperfections.

the Lieb-Robinson bound for short-ranged Hamiltonians [52]. In the thermodynamic limit $L \to \infty$ and at large times $uJt \gg 1$, L_c grows with a velocity $V = 2uJ/\pi$. In the presence of disorder, instead, we expect L_c to initially increase, as spins correlate within the localization length, and to saturate at long times due to AL. This experimental evidence proves that our Hamiltonian engineering technique can indeed introduce disorder in the system evolution. The figure also shows the behavior of L_c as the strength of the interactions [v in Eq. (3)] are varied, for a fixed disorder strength. The experiments clearly reveal the emergence of slow growth in L_c when interactions are added, the hallmark feature of MBL [15,53].

The strength and limitations of our experimental system are evident when we consider the change in L_c as a function of disorder strength for the noninteracting case (Fig. 4). Increasing disorder is clearly seen to result in a saturation of L_c, consistent with AL. The lines are numerical simulations, showing that experimental results are consistent with theoretical predictions. Discrepancies at higher L_c are likely due to experimental imperfections.

Control imperfection (such as pulse errors and rf transients) and decoherence due to the open system dynamics preferentially affect the higher quantum coherences of large spin correlations, leading to an apparent saturation of L_c. The same experimental imperfections make it even more difficult to observe the ergodic phase, where interactions dominate disorder, ideally leading to a fast growth in time of the correlation length, which is more heavily affected by the observed saturation. While high-fidelity experimental control of complex many-body states is key for any experimental metric of complexity, in some cases, it is still possible to distinguish between the saturation of L_c due to experimental limitations at long time and its quenching due to increasing disorder using

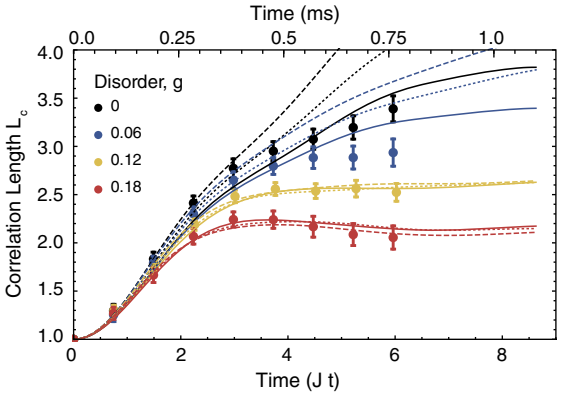

FIG. 4. Experimental correlations in noninteracting spin chains. Correlation length L_c for various strength $\propto g$ of disordered transverse fields, with $u = 0.24$ and $v = 0$ [Eq. (3)]. Errorbars are determined from the noise in the free induction decay. The lines are numerical simulations using 6 (solid), 10 (dotted), and 40 (dashed) spins, respectively, averaged over 126 disorder realizations.

additional symmetry properties of the MQCs (see Sec. 5 in Supplemental Material [24]).

Note that in the experiments we can probe this dynamics only for relatively short times, where the physical system is a good approximation to the ideal model, as verified elsewhere [21]. Indeed, while the average chain length (determined by crystal defects) is much longer than the 20–25 spins explored on these time scales, we have long-range couplings ($\propto 1/r^3$) in a 3D crystal, where each spin chain interacts with six surrounding chains. In addition, pulse imperfections and higher orders in the Magnus expansion can lead to unwanted terms in the engineered Hamiltonian. We note that rapidly applied rf pulses do not give rise to heating [54], while the unavoidable interaction with the environment, dominated by other spins in the system, leads to decoherence (dephasing) that affects equally the interacting and noninteracting regimes. We kept the experimental time short to minimize these effects and observe the localization regime, before the experimentally unavoidable thermalization can appear (indeed the time is also much shorter than the relaxation time $T_1 \approx 0.8$ s and the P dynamics).

We can obtain a more intuitive understanding of why our experimental method for extracting the correlation length from MQC is quite robust. While measuring L_c via the MQC is exact in the integrable case, this method can still be applied to MBL systems due to their "emergent integrability," characterized by a complete set of local integrals of motions (LIOMs) [16,17]. While the number of possible configurations ζ_k in these LIOMs is exponential, only a fraction of them (corresponding to small k) have significant weights—a consequence of area law entanglement in MBL systems [55,56]. Then, when applied to MBL systems, the MQC method approximately counts the L_c of these interacting LIOMs, while still exhibiting the same logarithmic growth as entanglement entropy. We can further understand our measurement in terms of OTOCs [32,57,58]. As explained in detail in Sec. 4 of the Supplemental Material [24], in order to extract the MQC intensities we effectively measure the quantities

$$S_\phi(t) = \mathrm{Tr}[\rho_{\mathrm{eq}}\Phi^\dagger(t)\rho_{\mathrm{eq}}\Phi(t)],$$
$$\text{with} \quad \Phi(t) = U(t)e^{i\phi\sum_j S_x^j}U^\dagger(t). \tag{4}$$

While we can only measure OTOCs for collective operators on the whole system, such as Φ, these OTOCs still give some information about the spreading or localization of correlations, since ρ_{eq} is a sum of local operators. The information is made more accurate as we consider an average of several OTOCs for different $\Phi(0)$ operators, even if we cannot measure a whole basis of a subsystem, as required to extract the EE [59,60]. It will be interesting to experimentally measure other OTOCs in our system, as OTOCs have been studied in the context of information scrambling in black holes [61,62] and disordered spin systems [32,57,63–66].

In conclusion, we introduced a novel metric for localization, able to distinguish between many-body and single-particle localization. The correlation metric can be measured experimentally, with the only requirement of collective rotations and measurements, by extending MQC techniques developed in NMR (which can as well be applied to many other physical systems [58]). We also reveal an interesting relationship between the protocol for measuring the correlation length and the measurement of OTOCs, thus further confirming its ability to measure the logarithmic growth of entanglement associated with MBL. Thanks to our control techniques, we were able to explore a broad range of interesting behaviors in this solid-state spin system. In particular, we observed, for the first time, many-body localization in a natural spin system associated with a single crystal at high temperature. We note that, while we interpreted our results mostly based on a simplified model (1D, nearest-neighbour couplings), the real system is more complex due to long-range interactions and a 3D structure. It will be thus interesting to use the tools developed in this work to study subtler properties of localization when these effects are highlighted by the experimental scheme.

We thank S. Choi, I. Marvian, S. Lloyd, and M. Lukin for insightful discussions. This work was supported in part by the U.S. Air Force Office of Scientific Research Grant No. FA9550-12-1-0292, the U.S. Office of Naval Research Grant No. N00014-14-1-0804, and by the National Science Foundation PHY0551153 and CHE1410504. C. R. acknowledges support of a Walter and Constance Burke Award from Dartmouth College.

*pcappell@mit.edu

[1] P. W. Anderson, Phys. Rev. **109**, 1492 (1958).
[2] D. S. Wiersma, P. Bartolini, A. Lagendijk, and R. Righini, Nature (London) **390**, 671 (1997).
[3] J. Billy, V. Josse, Z. Zuo, A. Bernard, B. Hambrecht, P. Lugan, D. Clement, L. Sanchez-Palencia, P. Bouyer, and A. Aspect, Nature (London) **453**, 891 (2008).
[4] G. Roati, C. D'Errico, L. Fallani, M. Fattori, C. Fort, M. Zaccanti, G. Modugno, M. Modugno, and M. Inguscio, Nature (London) **453**, 895 (2008).
[5] D. Basko, I. Aleiner, and B. Altshuler, Ann. Phys. (Amsterdam) **321**, 1126 (2006).
[6] D. M. Basko, I. L. Aleiner, and B. L. Altshuler, Phys. Rev. B **76**, 052203 (2007).
[7] R. Nandkishore and D. A. Huse, Annu. Rev. Condens. Matter Phys. **6**, 15 (2015).
[8] J. Smith, A. Lee, P. Richerme, B. Neyenhuis, P. W. Hess, P. Hauke, M. Heyl, D. A. Huse, and C. Monroe, Nat. Phys. **12**, 907 (2016).
[9] M. Schreiber, S. S. Hodgman, P. Bordia, H. P. Lüschen, M. H. Fischer, R. Vosk, E. Altman, U. Schneider, and I. Bloch, Science **349**, 842 (2015).
[10] J.-Y. Choi, S. Hild, J. Zeiher, P. Schauß, A. Rubio-Abadal, T. Yefsah, V. Khemani, D. A. Huse, I. Bloch, and C. Gross, Science **352**, 1547 (2016).
[11] A. Pal and D. A. Huse, Phys. Rev. B **82**, 174411 (2010).
[12] M. Serbyn and Z. Papić, and D. A. Abanin, Phys. Rev. X **5**, 041047 (2015).
[13] D. J. Luitz, N. Laflorencie, and F. Alet, Phys. Rev. B **91**, 081103 (2015).
[14] M. Žnidarič, T. Prosen, and P. Prelovšek, Phys. Rev. B **77**, 064426 (2008).
[15] J. H. Bardarson, F. Pollmann, and J. E. Moore, Phys. Rev. Lett. **109**, 017202 (2012).
[16] M. Serbyn, Z. Papić, and D. A. Abanin, Phys. Rev. Lett. **111**, 127201 (2013).
[17] D. A. Huse, R. Nandkishore, and V. Oganesyan, Phys. Rev. B **90**, 174202 (2014).
[18] R. Islam, R. Ma, P. M. Preiss, M. Eric Tai, A. Lukin, M. Rispoli, and M. Greiner, Nature (London) **528**, 77 (2015).
[19] V. Oganesyan and D. A. Huse, Phys. Rev. B **75**, 155111 (2007).
[20] M. Goihl, M. Friesdorf, A. H. Werner, W. Brown, and J. Eisert, arXiv:1601.02666.
[21] W. Zhang, P. Cappellaro, N. Antler, B. Pepper, D. G. Cory, V. V. Dobrovitski, C. Ramanathan, and L. Viola, Phys. Rev. A **80**, 052323 (2009).
[22] P. Cappellaro, C. Ramanathan, and D. G. Cory, Phys. Rev. Lett. **99**, 250506 (2007).
[23] P. Jordan and E. Wigner, Z. Phys. B **47**, 631 (1928).
[24] See Supplemental Material at http://link.aps.org/supplemental/10.1103/PhysRevLett.120.070501 for additional details on the theoretical model, simulations and experiments.
[25] E. B. Fel'dman and S. Lacelle, Chem. Phys. Lett. **253**, 27 (1996).
[26] E. Rufeil-Fiori, C. M. Sánchez, F. Y. Oliva, H. M. Pastawski, and P. R. Levstein, Phys. Rev. A **79**, 032324 (2009).
[27] U. Haeberlen and J. Waugh, Phys. Rev. **175**, 453 (1968).
[28] G. Kaur and P. Cappellaro, New J. Phys. **14**, 083005 (2012).
[29] Y.-S. Yen and A. Pines, J. Chem. Phys. **78**, 3579 (1983).
[30] A. Ajoy and P. Cappellaro, Phys. Rev. Lett. **110**, 220503 (2013).
[31] R. Fan, P. Zhang, H. Shen, and H. Zhai, Science bulletin **62**, 707 (2017).
[32] J. Li, R. Fan, H. Wang, B. Ye, B. Zeng, H. Zhai, X. Peng, and J. Du, Phys. Rev. X **7**, 031011 (2017).
[33] P. Hauke and M. Heyl, Phys. Rev. B **92**, 134204 (2015).
[34] Z. Huang, C. Macchiavello, and L. Maccone, Phys. Rev. A **94**, 012101 (2016).
[35] P. Hauke, M. Heyl, L. Tagliacozzo, and P. Zoller, Nat. Phys. **12**, 778 (2016).
[36] S. S. Kondov, W. R. McGehee, W. Xu, and B. DeMarco, Phys. Rev. Lett. **114**, 083002 (2015).
[37] M. Pasienski, D. McKay, M. White, and B. DeMarco, Nat. Phys. **6**, 677 (2010).
[38] G. A. Álvarez and D. Suter, Phys. Rev. Lett. **104**, 230403 (2010).
[39] M. Gärttner, P. Hauke, and A. M. Rey, arXiv:1706.01616 [Phys. Rev. Lett. (to be published)].
[40] B. Groisman, S. Popescu, and A. Winter, Phys. Rev. A **72**, 032317 (2005).

[41] G. De Tomasi, S. Bera, J. H. Bardarson, and F. Pollmann, Phys. Rev. Lett. **118**, 016804 (2017).
[42] P. Cappellaro, L. Viola, and C. Ramanathan, Phys. Rev. A **83**, 032304 (2011).
[43] C. Ramanathan, P. Cappellaro, L. Viola, and D. G. Cory, New J. Phys. **13**, 103015 (2011).
[44] U. Haeberlen, *High Resolution NMR in Solids: Selective Averaging* (Academic Press, New York, 1976).
[45] M. Munowitz and A. Pines, in *Principle and Applications of Multiple-Quantum NMR*, edited by I. Prigogine and S. Rice, Advances in Chemical Physics, Vol. 66 (Wiley, Hoboken, NJ, 1975).
[46] J. Baum, M. Munowitz, A. N. Garroway, and A. Pines, J. Chem. Phys. **83**, 2015 (1985).
[47] C. Ramanathan, H. Cho, P. Cappellaro, G. S. Boutis, and D. G. Cory, Chem. Phys. Lett. **369**, 311 (2003).
[48] J. Baum and A. Pines, J. Am. Chem. Soc. **108**, 7447 (1986).
[49] M. Munowitz, A. Pines, and M. Mehring, J. Chem. Phys. **86**, 3172 (1987).
[50] G. A. Álvarez, D. Suter, and R. Kaiser, Science **349**, 846 (2015).
[51] G. Bodenhausen, H. Kogler, and R. Ernst, J. Magn. Reson. **58**, 370 (1984).
[52] E. H. Lieb and D. W. Robinson, Commun. Math. Phys. **28**, 251 (1972).
[53] M. Pino, Phys. Rev. B **90**, 174204 (2014).
[54] D. A. Abanin, W. De Roeck, W. W. Ho, and F. Huveneers, Phys. Rev. B **95**, 014112 (2017).
[55] J. Eisert, M. Cramer, and M. B. Plenio, Rev. Mod. Phys. **82**, 277 (2010).
[56] B. Bauer and C. Nayak, J. Stat. Mech. (2013) P09005.
[57] Y. Huang, Y.-L. Zhang, and X. Chen, Ann. Phys. (Amsterdam) **529**, 1600318 (2017).
[58] M. Garttner, J. G. Bohnet, A. Safavi-Naini, M. L. Wall, J. J. Bollinger, and A. M. Rey, Nat. Phys. **13**, 781 (2017).
[59] P. Hosur, X.-L. Qi, D. A. Roberts, and B. Yoshida, J. High Energy Phys. 02 (2016) 004.
[60] R. Fan, P. Zhang, H. Shen, and H. Zhai, Science bulletin **62**, 707 (2017).
[61] B. Swingle, G. Bentsen, M. Schleier-Smith, and P. Hayden, Phys. Rev. A **94**, 040302 (2016).
[62] N. Y. Yao, F. Grusdt, B. Swingle, M. D. Lukin, D. M. Stamper-Kurn, J. E. Moore, and E. A. Demler, arXiv: 1607.01801.
[63] B. Swingle and D. Chowdhury, Phys. Rev. B **95**, 060201 (2017).
[64] R.-Q. He and Z.-Y. Lu, Phys. Rev. B **95**, 054201 (2017).
[65] X. Chen, T. Zhou, D. A. Huse, and E. Fradkin, Ann. Phys. (Amsterdam) **529**, 1600332 (2017).
[66] Y. Chen, arXiv:1608.02765.